International Journal of Computer Science and Information Technology
ISSN: 3005-9682 (Print), ISSN: 3005-7140 (Online) | Volume 8, Number 3, Year 2026
DOI: https://doi.org/10.62051/ijcsit.v8n3.09
Journal homepage: https://wepub.org/index.php/IJCSIT/index

An Improved YOLOv8n-Based Method for Ultrasonic Phased Array S-Scan Defect Detection in LPG Spherical Tank Welds

Zhuangzhuang Zhang, Zhaohua Liu, Bowen Yuan

College of Mechanical Engineering, Tianjin University of Technology and Education, Tianjin, China

ABSTRACT

To address the high missed-detection rate of traditional object detection methods caused by small defect sizes, irregular shapes, and low contrast in ultrasonic phased array S-scan images of LPG spherical tank welds, an improved YOLOv8n-based weld defect detection method is proposed. Building upon the lightweight architecture of YOLOv8n, a Multi-Level Channel Attention (MLCA) mechanism is introduced to enhance the model's capability in representing low-contrast and small-scale defect features. In addition, the C2f module is integrated with Deformable Convolution (DCNv3) during the feature extraction stage to construct a C2f-DCNv3 feature extraction module, thereby improving the model's ability to capture irregular weld defect characteristics. Experiments are conducted on an LPG spherical tank weld ultrasonic phased array S-scan image dataset. The results demonstrate that, compared with the original YOLOv8n and several mainstream object detection methods, the proposed approach achieves significant improvements in Precision, Recall, and mAP@0.5. Moreover, it satisfies the real-time requirements of engineering applications while maintaining high detection accuracy. The findings indicate that the proposed method provides an effective technical solution for intelligent ultrasonic inspection of LPG spherical tank welds.

KEYWORDS

Ultrasonic phased array; S-scan image; Weld defect detection; YOLOv8n

1. INTRODUCTION

LPG spherical tanks are critical pressure vessel structures widely used in petrochemical industries and energy storage and transportation systems. The integrity of their welded joints is directly associated with the operational safety and reliability of the entire equipment. During long-term service, weld regions are susceptible to various defects, such as cracks, lack of penetration, and porosity [1]. If these defects are not detected and addressed in a timely manner, they may lead to severe safety incidents. Therefore, efficient and reliable nondestructive testing (NDT) of LPG spherical tank welds is of significant importance for ensuring safe operation.

Phased array ultrasonic testing (PAUT) has been extensively applied in pressure vessel weld inspection owing to its high detection efficiency and intuitive imaging capability [2]. In particular, S-scan images can effectively visualize the spatial distribution of internal weld defects and are commonly used for on-site evaluation [3]. However, PAUT S-scan images often suffer from challenges such as small defect sizes, low signal-to-noise ratios, and complex background interference. As a result, defect identification largely depends on the experience of inspectors, and manual interpretation tends to be inefficient and subjective. These limitations hinder the application of traditional inspection methods in large-scale and intelligent inspection scenarios.

In recent years, with the rapid development of deep learning technologies, object detection methods based on convolutional neural networks (CNNs) have achieved remarkable success in industrial

Content from this work may be used under the terms of CC BY-NC 4.0 licence (https://creativecommons.org/licenses/by-nc/4.0/).
Published by Warwick Evans Publishing.

visual inspection tasks [4]. Previous studies have demonstrated that deep learning-based approaches exhibit strong potential in weld defect recognition, metallic surface defect detection, and industrial nondestructive evaluation. Among them, classical object detection frameworks such as Faster R-CNN [5] and YOLO [6] have been widely applied to weld defect detection and casting defect identification, achieving promising detection performance [7]. With the continuous evolution of the YOLO family of models, YOLOv8-based weld defect detection methods have gradually attracted increasing research attention. For instance, Chen et al. proposed the YOLOv8-ELA algorithm for weld defect detection, achieving improved detection accuracy and robustness [8]. Zhang et al. developed the YOLOv8-WD model for industrial weld defect detection, which significantly enhanced detection accuracy [9]. Wang et al. introduced a lightweight YOLOv8-DPE network that enables efficient weld defect detection [10]. Nevertheless, PAUT S-scan images differ significantly from natural images in terms of imaging mechanisms and feature distributions. Consequently, directly applying general-purpose object detection models often results in suboptimal performance, particularly for detecting small and low-contrast weld defects, where the miss-detection rate remains relatively high.

YOLOv8, as a new-generation single-stage object detection framework, incorporates several improvements in network architecture and training strategies, achieving a favorable balance between detection accuracy and real-time performance [11]. Among its variants, YOLOv8n features a lightweight architecture with fewer parameters and faster inference speed, making it particularly suitable for deployment in practical engineering scenarios. However, when applied to phased array ultrasonic S-scan images containing irregularly shaped and weak-feature weld defects, its feature representation capability remains insufficient.

To address these challenges, this study proposes an improved YOLOv8n-based method for weld defect detection in phased array ultrasonic S-scan images of LPG spherical tanks. Specifically, a multi-level channel attention mechanism (MLCA) is introduced to enhance the model's sensitivity to small and low-contrast defects. In addition, deformable convolution (DCNv2/3) [12] is integrated into the C2f module to improve the network's spatial modeling capability for irregular weld defects. Experimental results on a PAUT S-scan image dataset of LPG spherical tank welds demonstrate that the proposed method outperforms several mainstream detection models in terms of detection accuracy and recall, indicating its strong potential for practical engineering applications.

Furthermore, the proposed framework maintains stable detection performance under complex background interference and varying defect scales, highlighting its robustness and effectiveness for real-world nondestructive inspection scenarios.

2. IMPROVED YOLOV8N-BASED WELD DEFECT DETECTION METHOD

2.1. Overview of the YOLOv8n Network Architecture

The YOLO (You Only Look Once) series of algorithms are single-stage object detection methods that have the advantages of fast detection speed and end-to-end training. They have been widely applied in the field of industrial visual inspection [6]. YOLOv8 is a new-generation object detection model proposed by Ultralytics, which introduces several improvements in network architecture and training strategies compared with previous versions [11].

YOLOv8 adopts an anchor-free detection mechanism, which directly predicts the center points and bounding box sizes of targets. This approach avoids the hyperparameter tuning problems caused by anchor box design and improves detection stability and generalization capability to a certain extent [13]. The overall network architecture mainly consists of three components: Backbone, Neck, and Head. The Backbone is responsible for extracting multi-scale features from the input images, the Neck enhances semantic information through feature fusion, and the Head performs the prediction of object categories and bounding box locations.

Considering the requirements of real-time performance and model lightweight deployment for phased array ultrasonic S-scan image detection of LPG spherical tank welds, YOLOv8n is selected as the baseline model in this study. While maintaining a high detection speed, targeted improvements are introduced to enhance its capability for detecting small-sized and low-contrast weld defects.

2.2. Overall Architecture of the Improved Model

To address the challenges of small target size, irregular morphology, and insufficient feature representation in ultrasonic phased array S-scan images, an improved defect detection model is proposed based on the YOLOv8n architecture.

In the Backbone stage, the original C2f modules are replaced with C2f-DCNv3 modules that incorporate Deformable Convolution (DCNv3), thereby enhancing the network's ability to model irregular defect morphologies. In addition, the MLCA attention mechanism is introduced at key feature fusion locations between the Backbone and Neck to jointly model channel and spatial information, thus highlighting discriminative features in weld defect regions.

The improved model effectively enhances detection precision and recall for complex weld defects while maintaining the lightweight characteristics and real-time performance of YOLOv8n. Moreover, the integration of attention mechanisms and deformable convolution improves feature representation capability and strengthens the robustness of the model when handling low-contrast and small-scale defects. The overall architecture still follows an end-to-end detection framework, facilitating practical engineering deployment.

2.3. Design of the MLCA Attention Mechanism

In ultrasonic phased array S-scan images, weld defects typically appear as small-scale targets with subtle grayscale variations and strong background interference. During feature extraction, conventional convolutional neural networks are prone to being affected by irrelevant background information, which may weaken critical defect features. To address this issue, a Multi-Level Channel Attention (MLCA) mechanism is introduced to enhance the model's ability to focus on discriminative features.

The MLCA mechanism models channel-wise weights across multi-scale features, emphasizing informative channels related to defect regions while preserving feature diversity. Specifically, MLCA first applies global average pooling to the input feature maps to obtain global statistical information for each channel. Then, a multi-layer perceptron structure is employed to perform weighted fusion of channel features from different levels, generating channel attention weights. Finally, these weights are applied to the original feature maps to enhance important features.

Compared with conventional attention mechanisms such as SE and CBAM, MLCA can more effectively exploit multi-scale feature information and demonstrates superior feature selection capability in low-contrast and small-target scenarios. By integrating MLCA into the YOLOv8n network, the model achieves more accurate localization of weld defect regions under complex background conditions. The overall architecture of the MLCA module is illustrated in Fig. 1.

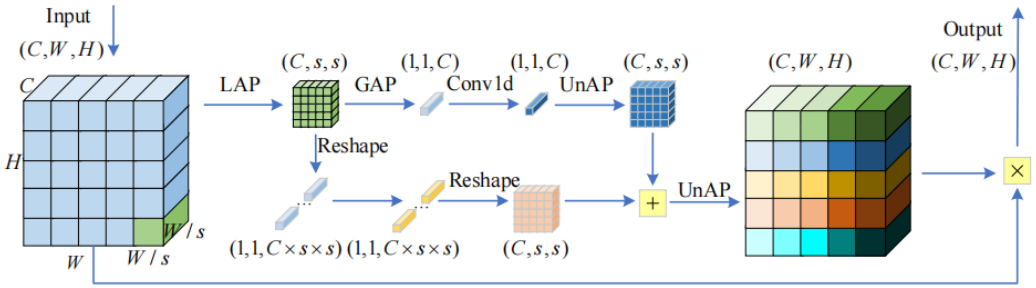

Figure 1. Structure of the MLCA module

2.4. C2f-DCNv3 Feature Extraction Module

In ultrasonic phased array S-scan images, weld defects often exhibit diverse morphologies and blurred boundaries. Conventional convolution with fixed sampling locations is insufficient to effectively capture such irregular features. Deformable Convolution introduces learnable offsets into the convolution operation, enabling the sampling positions of the convolution kernel to adapt dynamically to feature variations, thereby improving the modeling capability for geometrically deformed targets.

In this study, the latest DCNv3 module is adopted and embedded into the C2f structure of YOLOv8n to construct a C2f-DCNv3 feature extraction module. DCNv3 optimizes the offset modeling mechanism while maintaining computational efficiency, resulting in more stable training behavior and enhanced spatial modeling capability. The structural principle of the deformable convolution operation is illustrated in Fig. 2.

Within the C2f-DCNv3 module, part of the standard convolution operations are replaced with DCNv3, allowing the network to dynamically perceive morphological variations of weld defects during feature extraction. This design preserves the original advantages of the C2f module, including feature reuse and lightweight characteristics, while enhancing the network's adaptability to irregular weld defects.The detailed architecture of the proposed C2f-DCNv3 module is presented in Fig. 3.

By incorporating the C2f-DCNv3 module, the proposed model effectively improves the detection performance for complex weld defects such as cracks and lack of penetration, without significantly increasing the number of parameters or computational complexity.Furthermore, the enhanced spatial adaptability enables the network to capture subtle defect features under complex background conditions, thereby improving detection robustness in practical inspection

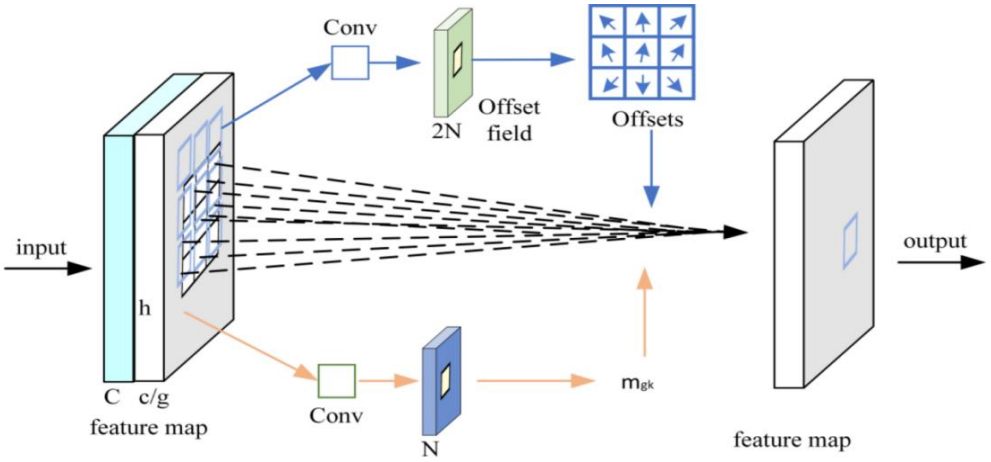

Figure 2. Structure of the deformable convolution module

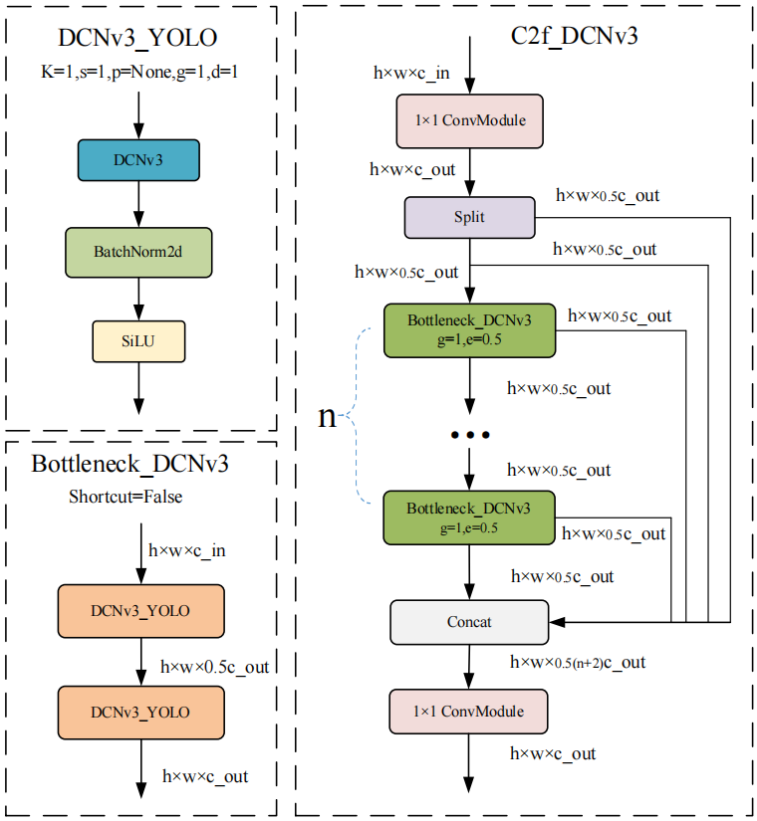

Figure 3. Structure of the C2f-DCNv3 module

3. EXPERIMENTS AND RESULTS ANALYSIS

3.1. Dataset Description

The dataset used in this study was collected from on-site ultrasonic phased array inspections of LPG spherical tank welds. During the inspection process, phased array ultrasonic equipment was employed to acquire S-scan images of the weld regions. The defect types and locations were annotated by experienced nondestructive testing (NDT) professionals to ensure labeling accuracy and engineering reliability.

The dataset includes various common types of weld defects, such as cracks, lack of penetration, porosity, and slag inclusions. Since defects in ultrasonic phased array S-scan images typically appear as small-sized and low-contrast feature regions, the dataset exhibits pronounced small-object detection characteristics. Representative examples of different weld defect types in the collected S-scan images are shown in Fig. 4.

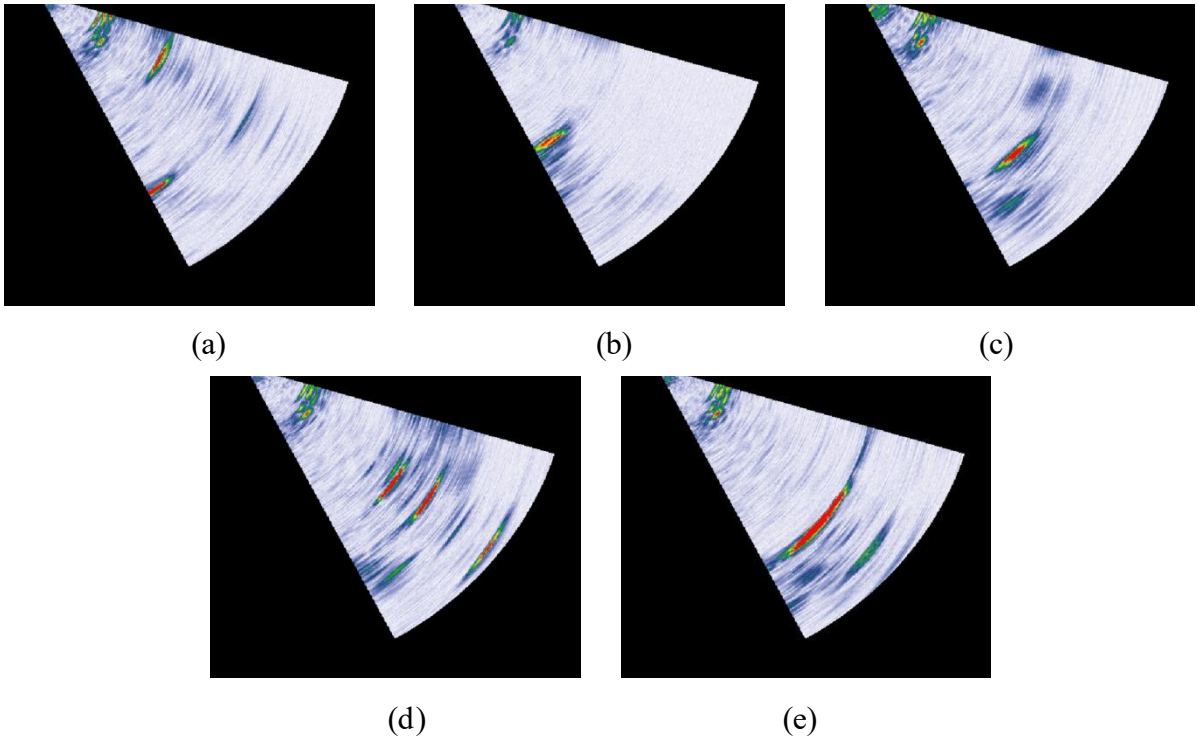

Figure 4. Phased array ultrasonic S-scan images of weld defects: (a) slag inclusion; (b) crack; (c) porosity; (d) lack of penetration; (e) lack of fusion

To improve the generalization capability of the model, data augmentation techniques were applied to the original dataset, including random flipping, scale transformation, and brightness perturbation. After augmentation, the number of samples in each defect category was significantly increased to enhance data diversity and class balance. The numbers of images before and after augmentation are summarized in Table 1.

Table 1. Dataset of ultrasonic phased array S-scan images before and after data augmentation

Dataset	Slag Inclusion	Crack	Lack of Fusion	Lack of Penetration	Porosity	Total
Original images	360	360	360	360	360	1800
Augmented images	800	800	800	800	800	4000

The augmented image dataset was randomly shuffled and then divided into training, validation, and test sets at a ratio of 7:2:1. The detailed data partition is presented in Table 2.

Table 2. Partition of the Ultrasonic Phased Array S-Scan Image Dataset

Dataset	Number of Images	Proportion (%)
Training set	2800	70
Validation set	800	20
Test set	400	10

3.2. Experimental Environment and Parameter Settings

The experiments were conducted under the following hardware and software configurations. In terms of hardware, the experimental platform was equipped with a 12th Gen Intel(R) Core (TM) i7-12700KF processor and an NVIDIA GeForce RTX 3090 GPU, running on a 64-bit Windows 11 operating system. For the software environment, the deep learning framework was built based on Anaconda, using PyTorch 1.8.1, with Python version 3.8.13.

During model training, the input image resolution was set to 640 × 640 × 3, the number of training epochs was 300, and the batch size was 4. The SGD (Stochastic Gradient Descent) optimizer was adopted, with an initial learning rate (lr0) of 0.01, a final learning rate factor (lrf) of 0.01, momentum of 0.937, and a weight decay coefficient of 0.0005. These parameter settings provide a stable computational environment and optimization basis for model training and experimental evaluation.

3.3. Evaluation Metrics

To comprehensively evaluate the performance of the model in the weld defect detection task, Precision, Recall, and mAP@0.5 were selected as the main evaluation metrics. Precision measures the accuracy of the detection results, while Recall reflects the ability of the model to identify actual defect targets. The mAP@0.5 metric comprehensively evaluates the overall detection performance of the model across different categories. The calculation formulas are as follows:

$$\mathrm{Pr}ecision = \frac{TP}{TP + FP} \tag{1}$$

$$\mathrm{Re}call = \frac{TP}{TP + FN} \tag{2}$$

Where TP, FP, and FN denote true positives, false positives, and false negatives, respectively. In object detection tasks, the Average Precision (AP) is calculated from the Precision–Recall (P–R) curve, and the mean Average Precision (mAP) is obtained by averaging the AP values of all categories. The expression is as follows

$$mAP = \frac{1}{N}\sum_{i=1}^{N} AP_i \tag{3}$$

Where N denotes the number of categories. In addition, to evaluate the real-time performance of the model, the frames per second (FPS) is used as the detection speed metric, and its calculation formula is as follows:

$$FPS = \frac{N}{T} \tag{4}$$

Where N represents the number of processed images, and T denotes the total processing time.

3.4. Ablation Study Analysis

To verify the effectiveness of the MLCA attention mechanism and the C2f-DCNv3 module in improving the YOLOv8n network, several ablation experiments were conducted. The experimental results are shown in Table 3.

Table 3. Ablation Study Results

Model	MLCA Attention	C2f-DCNv3	P (%)	R (%)	mAP@0.5 (%)
YOLOv8n	×	×	86.2	78.5	82.8
Model 1	√	×	87.8	82.4	86.5
Model 2	×	√	89.1	80.7	87.3
Improved YOLOv8n	√	√	90.5	84.6	88.2

The ablation experiments include four configurations: the original YOLOv8n model, a model with only the MLCA attention mechanism, a model with only the C2f-DCNv3 module, and the complete model incorporating both improvements. By comparing the detection performance of different models on the test set, the contribution of each improvement module to the overall performance can be clearly analyzed. This experimental design allows a systematic evaluation of the effectiveness of each component and helps reveal how different modules influence the feature extraction capability of the network.

The experimental results show that after introducing the MLCA attention mechanism, the Recall metric is significantly improved, indicating that this module can effectively enhance the model's ability to perceive low-contrast small defects. This improvement suggests that the attention mechanism can better highlight important defect-related features while suppressing irrelevant background information. After introducing the C2f-DCNv3 module, the mAP@0.5 metric is further improved, demonstrating that deformable convolution helps improve the detection accuracy of irregular weld defects. When both modules are incorporated simultaneously, the model achieves the best results in Precision, Recall, and mAP@0.5, verifying the effectiveness of the proposed improvements and confirming the complementary advantages of the two modules.

3.5. Comparative Experiment Analysis

To further verify the superiority of the proposed method, the improved YOLOv8n model was compared with several mainstream object detection algorithms, including YOLOv5, YOLOv7-tiny, and Faster R-CNN. All models were trained and tested on the same dataset and under the same experimental settings to ensure a fair comparison. The detection performance of the model with different attention mechanisms is presented in Table 4. These comparative experiments provide a comprehensive evaluation of the proposed model and demonstrate its effectiveness in improving weld defect detection performance under complex inspection conditions.

Table 4. Performance comparison with other detection algorithms

Model	P (%)	R (%)	mAP@0.5 (%)	FPS
YOLOv8n	86.2	78.5	82.8	100
Faster R-CNN	85.2	68.3	77	11
YOLOv5n	76	70.1	78.5	138
YOLOv5s	74.6	73.8	78.9	115
YOLOv7-tiny	86.7	79.2	84.5	105
Improved YOLOv8n	90.5	84.6	88.2	100

The comparative results show that the traditional two-stage detection algorithm Faster R-CNN achieves relatively high detection accuracy but suffers from slow detection speed, making it difficult to meet the real-time requirements of on-site inspection. Although YOLOv5 and YOLOv7-tiny perform well in terms of detection speed, their recall rates for small weld defects remain insufficient, which may lead to missed detections in practical applications. In contrast, the improved YOLOv8n model proposed in this study achieves the best performance in both Recall and mAP@0.5 while maintaining high detection speed. This demonstrates its clear advantage in detecting small weld defects and effectively reducing the missed detection rate. The experimental results indicate that the proposed improvements enable the model to better capture subtle defect features and enhance the robustness of detection under complex background conditions. Furthermore, the improved balance between detection accuracy and computational efficiency highlights the practical value of the proposed model for real-time industrial inspection tasks.

3.6. Visualization Analysis of Detection Results

To intuitively demonstrate the practical detection performance of the improved model on ultrasonic phased-array S-scan images of LPG spherical tank welds, representative defect samples from the test set were selected for qualitative analysis. A visual comparison between the detection results of the original YOLOv8n model and the improved YOLOv8n model was conducted, as shown in Fig. 5. The visualization results provide a direct illustration of the model's ability to accurately identify and localize different types of weld defects. By comparing the predicted bounding boxes and confidence scores, the advantages of the improved model in detecting small-scale and low-contrast defects can be clearly observed. In particular, the improved model demonstrates more precise localization, fewer missed detections, and stronger feature response in complex background conditions. These results further verify the effectiveness of the proposed improvements in enhancing the detection capability of the model for subtle weld defects.

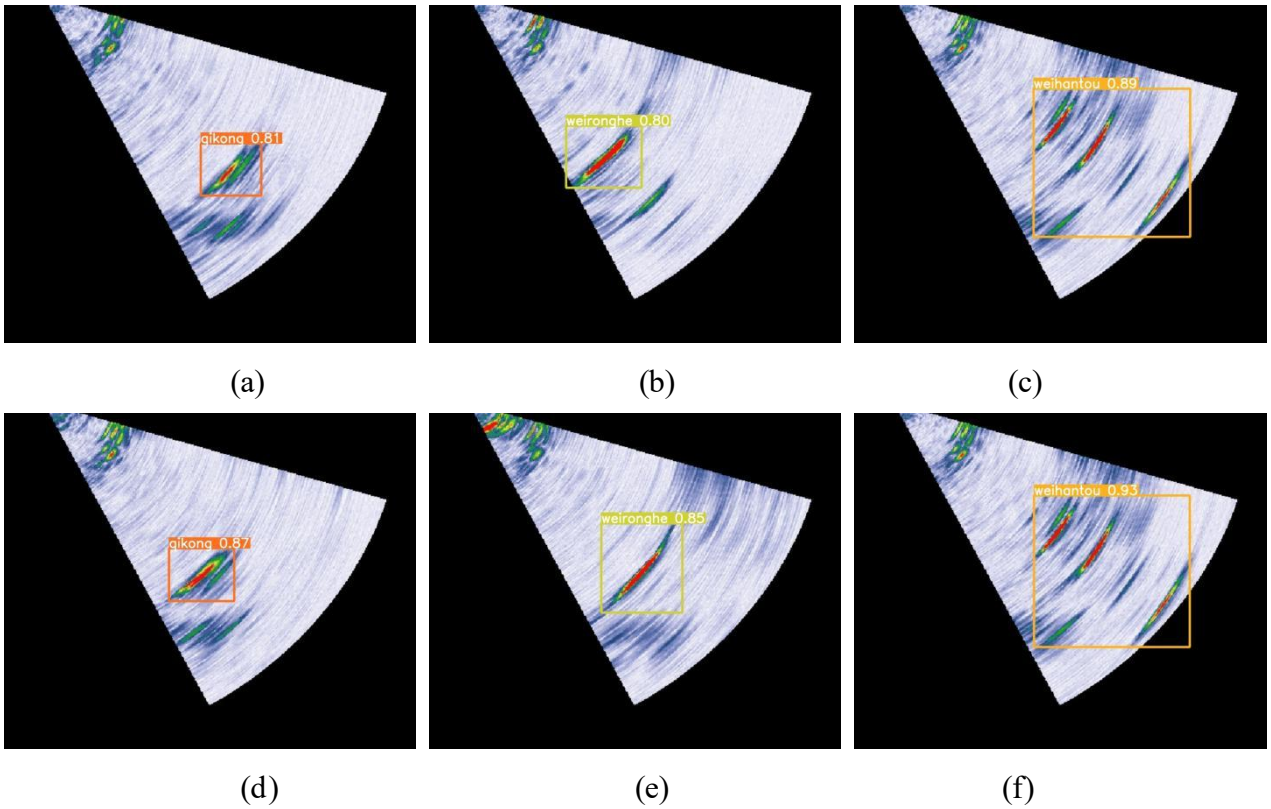

Figure 5. Visualization comparison of detection results before and after model improvement: (a-c) detection results of the original YOLOv8n model; (d-f) detection results of the improved YOLOv8n model

As shown in Fig. 5, for typical weld defect samples such as porosity, lack of fusion, and lack of penetration, the original YOLOv8n model can detect the main defect regions; however, when dealing with small-sized defects or defects with blurred boundaries, it exhibits problems such as bounding box deviation, inaccurate localization, and relatively low confidence scores. For example, in the porosity defect sample, the detection confidence of the original model ranges from 0.81 to 0.87, and the predicted bounding boxes show certain deviations from the actual defect regions.

In contrast, the improved YOLOv8n model produces more stable detection results on the same samples, with higher overlap between the predicted bounding boxes and the defect regions and more accurate boundary localization. Meanwhile, the overall confidence scores are improved. For instance, the confidence score for the lack-of-penetration defect increases from 0.89 in the original model to 0.93 in the improved model, indicating that the improved model responds more effectively to key defect features.

By combining the visualization results with the quantitative analysis presented earlier, it can be observed that the improved model demonstrates stronger feature representation capability and more stable detection performance under complex background conditions, further validating the effectiveness of the proposed improvements and their potential for engineering applications.

4. CONCLUSION

To address the challenges of small defect size, irregular shapes, and high missed-detection rates in ultrasonic phased-array S-scan images of LPG spherical tank welds, this paper proposes a weld defect detection method based on an improved YOLOv8n model. By introducing the MLCA attention mechanism and the C2f-DCNv3 feature extraction module into the network, the model's ability to capture features of low-contrast small defects and irregular defects is significantly enhanced.

Experimental results demonstrate that, compared with the original YOLOv8n and several mainstream detection methods, the proposed approach achieves significant improvements in Precision, Recall, and mAP@0.5, while maintaining good detection speed. Therefore, it can meet the dual requirements of accuracy and real-time performance in practical engineering applications.

In summary, the proposed method shows promising application prospects in ultrasonic phased-array inspection of LPG spherical tank welds, providing an effective technical approach for the intelligent development of weld nondestructive testing (NDT).

REFERENCES

[1] Kou S. Welding Metallurgy [M]. 2nd ed. Hoboken: Wiley, 2003.

[2] Drinkwater B W, Wilcox P D. Ultrasonic arrays for non-destructive evaluation: A review [J]. NDT & E International, 2006.

[3] Blitz J, Simpson G. Ultrasonic Methods of Non-Destructive Testing [M]. Chapman & Hall, 1996.

[4] LeCun Y, Bengio Y, Hinton G. Deep learning [J]. Nature, 2015.

[5] Ren S, He K, Girshick R. Faster R-CNN: Towards real-time object detection [J]. IEEE TPAMI, 2017.

[6] Redmon J, Farhadi A. YOLOv3: An incremental improvement [J]. arXiv, 2018.

[7] Zhang W, Yang D, Wang H. Data-driven methods for industrial defect detection [J]. IEEE TII, 2020.

[8] Chen Y, He Y, Wu L. Detection of welding defects using the YOLOv8-ELA algorithm [J]. Applied Sciences, 2025.

[9] Zhang X, Li Y, Chen H. YOLOv8-WD: Deep learning-based detection of weld defects [J]. Applied Sciences, 2024.

[10] Wang H, Liu Y, Zhao Q. YOLOv8-DPE: A lightweight object detection network for weld defect detection [J]. Welding in the World, 2025.

[11] Jocher G, et al. Ultralytics YOLOv8 [EB/OL]. 2023.

[12] Zhu X, Su W, Lu L. Deformable ConvNets v2: More deformable, better results [C]. CVPR, 2019.

[13] Tian Z, Shen C, Chen H. FCOS: Fully convolutional one-stage object detection [C]. ICCV, 2019.